Received: 30 March 2018 | Revised: 15 May 2018 | Accepted: 16 May 2018

DOI: 10.1002/jccs.201800120

JOURNAL OF THE CHINESE CHEMICAL SOCIETY

ARTICLE

N-propylbenzoguanamine sulfonic acid-functionalized magnetic nanoparticles: A novel and magnetically retrievable catalyst for the synthesis of 1,4-dihydropyridine derivatives

Masoumeh Gholami Dehbalaei[1] | Naser Foroughifar[1] | Alireza Khajeh-Amiri[2] | Hoda Pasdar[1]

[1]Department of Chemistry, Tehran North Branch, Islamic Azad University, Tehran, Islamic Republic of Iran

[2]Biomaterial Laboratory, Toxin Research Institute, Aja University of Medical Sciences, Tehran, Islamic Republic of Iran

Correspondence
Naser Foroughifar, Department of Chemistry, Tehran North Branch, Islamic Azad University, Tehran, Islamic Republic of Iran.
Email: n_foroughifar@yahoo.com

Funding information
Islamic Azad University-Tehran North Branch; Research Council of Aja University of Medical Sciences

The catalytic activity of *N*-propylbenzoguanamine sulfonic acid stabilized on silica-coated nano-Fe_3O_4 particles (Fe_3O_4/SiO_2-*N*-propyl-benzoguanamine-SO_3H) were proven to be as a novel magnetic solid acid catalyst for the synthesis of 1,4-dihydropyridine derivatives in a one-pot pseudo-four-component condensation reaction of barbituric acid, aromatic aldehydes, and ammonium acetate or aniline with high yield and short reaction times. The structure and magnetic properties of the obtained nanoparticles were characterized via Fourier transform infrared spectroscopy (IR), field emission scanning electron microscopy (FE-SEM), transmission electron microscope (TEM), energy dispersive X-ray analysis (EDXA), X-ray diffraction (XRD), thermogravimetry analysis (TGA), differential thermal analysis (DTA) and vibrating sample magnetometry (VSM), atomic absorption spectroscopy (AAS), and inductively coupled plasma–mass spectrometry (ICP-MS). The results demonstrated that the average size of the synthesized magnetite nanoparticles is about 25 nm. In addition, the heterogeneous catalyst can be easily recovered magnetically and can be reused for further runs without significant loss of its catalytic activity.

KEYWORDS

1,4-dihydropyridine, barbituric acid, green chemistry, hantzsch reaction, heterogeneous catalyst, MNPs–NPBG–SA

1 | INTRODUCTION

The heterogeneous catalysts composed of hybrid organic and inorganic materials have recently garnered interest from researchers as they possess the advantages of both homogeneous and heterogeneous catalysts.[1–4] The homogeneous catalysts are more active than heterogeneous catalysts. Due to solubility in reaction, homogeneous catalysts increase the catalyst bed, but use of these catalysts may not always result in the pure product of a reaction, and recycling of homogeneous catalysts is a boring and time-consuming task.[5] Many investigations have focused on heterogeneous catalysts, especially magnetic nanoparticles (MNPs), for example, nanoparticles Fe_3O_4.[6–9] This issue is due to their unique physical, electronic, and magnetic properties, in them including high-level area, low toxicity, good stability, ease of preparation, and recycling by means of an external magnetic field.[10] One can refer to the highly diversified applications of these materials, including the isolation of metallic ions,[11] magnetic resonance imaging (MRI),[12] drug transfer system,[13] isolation of protein,[14] and treatment of cancer.[15] MNPs of ferric oxide demonstrate highly chemical activity and are oxidized easily in air; therefore, this leads to the lose of magnetic properties and dispersion of magnetite. Thus, the creation of an appropriate surface coating is crucially important in order to restore the stability of the nanoparticles of magnetic ferric oxide.[16] From an applied viewpoint, in many cases, the protective shells not only cause stability in MNPs of ferric oxide but may also include some other uses.[17–20] The Fe_3O_4 is usually coated by a protective layer of silica with (Fe_3O_4/

SiO_2) structure for better improvement and the prevention of the accumulation of ferric oxide particles.[21,22] Specifically, catalysts of various MNPs are widely utilized in organic reactions. Recently, many kinds of inorganic nanomaterials with various combinations, physical aspects, and functionalities have been widely synthesized. Among these nanoparticles, highly biocompatible coordination polymer (Prussian Blue) nanoparticles with a hollow space and open pores in the shell are used as an anticancer drug and to deliver drugs, with potential for diagnostic and imaging applications. Therefore, the development of new, hollow, inorganic nanoparticles as potential drug nanocarriers is scientifically important and technologically useful for biomedical applications.[23] CAT@ZIF-90 composites can be applied in several fields and includes a size-sheltering function to catalase and protects catalase from the inhibitor proteinase K, biomolecular delivery, size-selective enzyme catalysis, and industrial wastewater treatment.[24] MSNs nanoparticles with other metals, metal oxides, and polymers would create new MSN-based hybrids that have the potential for many emerging biomedical tools and would help increase the loading of hydrophobic drugs and control the release timing of the loaded drugs for drug delivery application.[25] Mesoporous titania nanoparticles (MTNs) have been successfully applied in various fields for photoelectronic applications, photocatalysts to solve universal energy problems, intracellular imaging, sensors, separation, and fast mass transport.[26,27] By reducing the number of synthetic phases and using a small amount of side product with a shorter time of production, Multicomponent reactions (MCRs) have emerged as an important and effective tool.[28] Five and six-member heterocyclic compounds have drawn noticeabe attention from the pharmaceutical chemistry. These compounds show remarkable medicinal activity through bioactive compounds, and their synthetic methods have been noticed by pharmaceutical chemists. The Hantzsch reaction is a classic technique in the synthesis of 1,4-dihydropyridine, including a condensation reaction from an aldehyde and 1,3-dicarbonyl and NH_3.[29]

Several techniques have been adapted for the synthesis of dihydropyridine (DHP) using various catalysts, such as metal triflate catalyst,[30] nano-$ZnFe_2O_4$,[31] ionic liquid,[32] $InCl_3$,[33] 3D printed α-Al_2O_3,[34] and MNPs-BPAT,[35] and without catalysts,[36] such as I_2,[37] lanthanide oxide,[38] $SiO_2/HClO_4$,[39] and CAN.[40]

1,4-DHP compounds possess various biological and medicinal properties including blocking of calcium canal and antitumor activity, antisclerotic activities,[41] antidiabetic,[42] anti-inflammatory, and analgesic properties[43] and for the treatment of cardiovascular diseases.[44] Barbituric acid (hexahydropyrimidine-2,4,6-trione) is the structural basis for several drugs, for example, antispasmodic, soporific, anticonvulsant, anesthetic, and antitumor drugs.[45–48] It is worth noting that the synthesis of new derivatives of 1,4-dihydropyridine from barbituric acid may be assumed to be important in both theoretical and practical approaches.

This study has examined the synthesis of new derivatives of 1,4-dihydropyridine using barbituric acid, aromatic aldehydes, and ammonium acetate or aniline in the presence of MNPs with an acidic factor *N*-propylbenzoguanamine sulfonic acid stabilized on silica-coated nano-Fe_3O_4 particles (MNP–NPBG–SA) as a new and efficient catalyst with recycling potential and reusability. The MNP-NPBG-SA catalyst was prepared by chemical co-precipitation according to the previous literature.[49] The new derivatives of 1,4-DHP have been produced with high efficiency and at a minimum reaction time (Scheme 1). This is the first report presented about the synthesis of MNP-NPBG-SA, and it has been suggested that this catalyst could be applied to reactions such as Hantzsch reaction,[2] Michael addition,[50] and others.

2 | RESULTS AND DISCUSSION

2.1 | Characterization of novel MNP—NPBG–SA catalyst

MNP–NPBG–SA nanoparticles were characterized by fourier transform infrared (FT-IR) spectroscopy, X-ray diffraction (XRD), EDAX, transmission electron microscope (TEM), field emission scanning electron microscopy (FE-SEM), thermogravimetry analysis (TGA), vibrating sample magnetometry (VSM), inductively coupled plasma–mass spectrometry

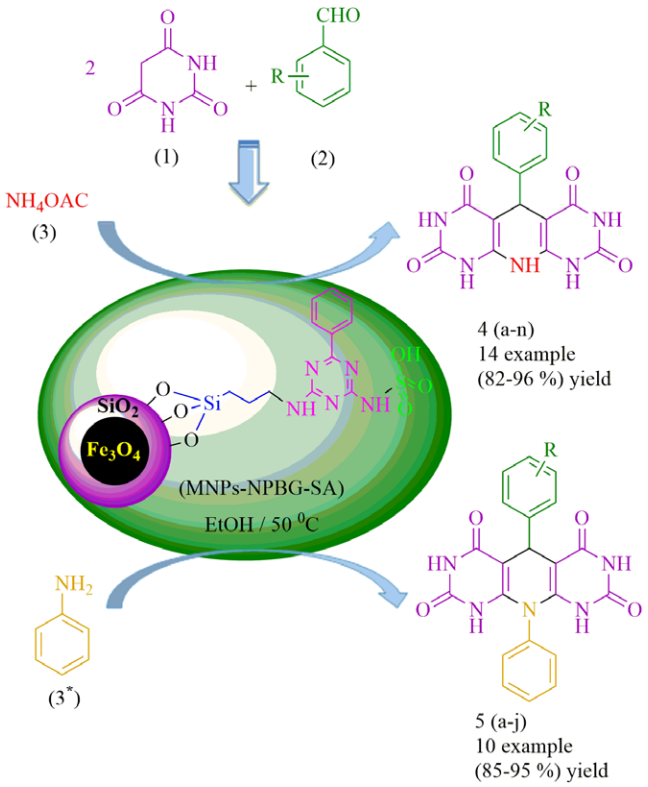

SCHEME 1 Synthesis of 1,4-dihydropyridine derivatives using novel MNP–NPBG–SA as a catalyst

(ICP-MS), and AAS techniques.[44] Figure 1 illustrates the FT-IR spectra for Fe_3O_4 nanoparticles, Fe_3O_4/SiO_2, Fe_3O_4/SiO_2/*N*-Propyl-Cl, Fe_3O_4/SiO_2/*N*-propyl/benzoguanamine and MNP–NPBG–SA.

Spectrum 1a shows the FT-IR spectrum of Fe_3O_4 nanoparticles at a stretching vibration of around 3,402 and 579 cm^{-1}, which combines the contributions from both symmetrical and asymmetrical modes of the surface hydroxyl groups and Fe–O bonds of iron oxide, respectively (Figure 1a). Spectrum 1b of Fe_3O_4/SiO_2 shows a peak at around 1,084 cm^{-1} which is assigned to the Si–O group and confirms that the formation of the SiO_2 shell and a weak peak at 1,625 cm^{-1} (twisting vibration mode of H–O–H absorbed in the silica shell) are obvious in the spectrum. In spectrum 1c–e, the presence of the anchored methylene groups is identified by the weak bands at 2,920 and 3,082 cm^{-1}, related to C–H symmetric and asymmetric stretching modes. In addition, peaks appear in the range 1,495–1,660 cm^{-1} (C–N in heterocyclic rings) and 3,174–3,410 cm^{-1} (stretching N–H) indicate the bond formation of benzoguanamine with Fe_3O_4/SiO_2/N-Propyl-Cl (Figure 1d). In the FT-IR spectra of MNP—NPBG–SA (spectrum 1e), the presence of the attached sulfonic acid by a broad peak at 3,692 cm^{-1} is confirmed. According to the results, the functional groups on the surface of the MNPs are grafted properly.

FE-SEM images of MNP–NPBG–SA nanoparticles are shown to determine the size of morphology (Figure 2). The diameter of particles is about 25 nm in a spherical shape.

Energy dispersive X-ray spectrometry (EDAX) was investigated to determine the kinds of elements in MNP–NPBG–SA. The EDAX result is obtained from the SEM image, and it has been demonstrated in the SEM highlighting zone. EDAX analysis obviously shows the presence

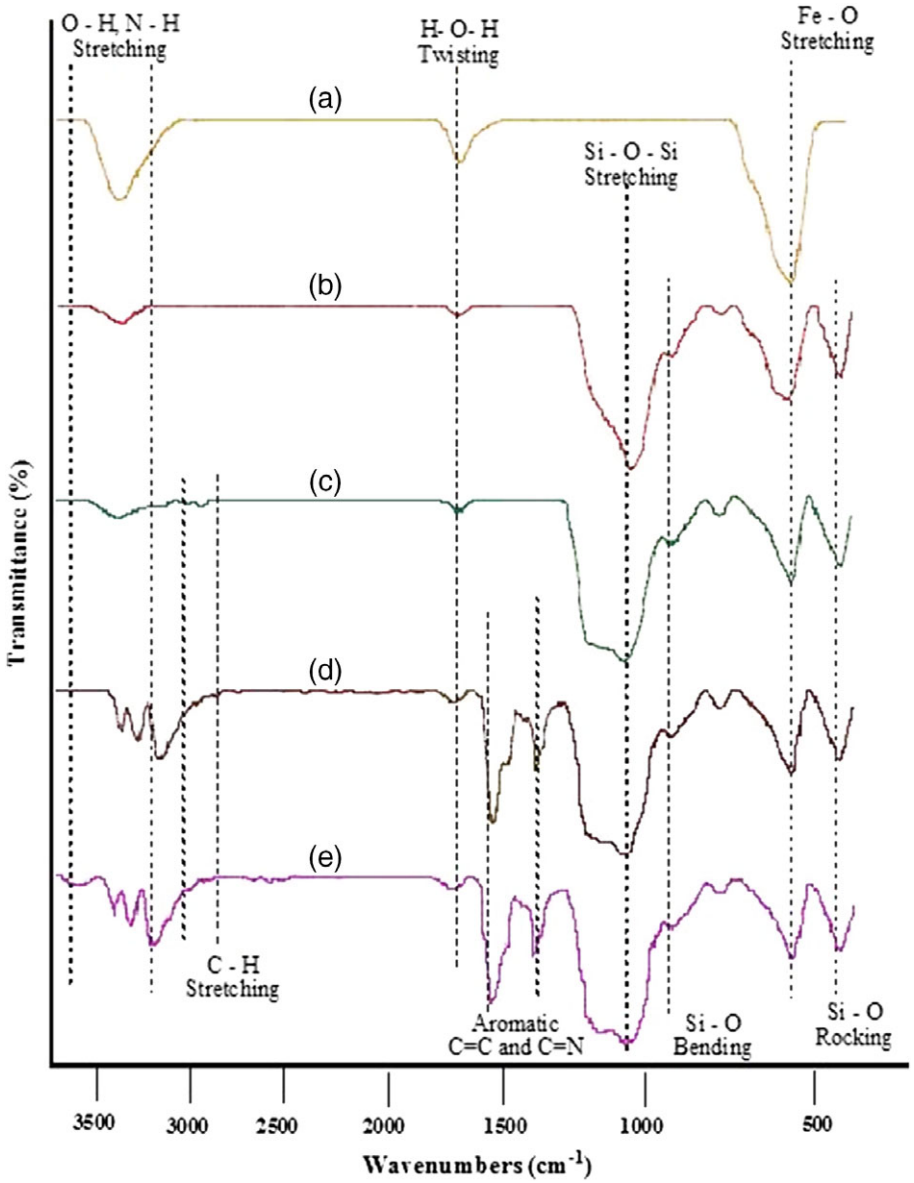

FIGURE 1 Comparison of FT-IR spectra for (a) Fe_3O_4, (b) Fe_3O_4/SiO_2, (c) Fe_3O_4/SiO_2/*N*-propyl-cl, (d) Fe_3O_4/SiO_2/*N*-propyl/benzoguanamine and (e) MNP–NPBG–SA

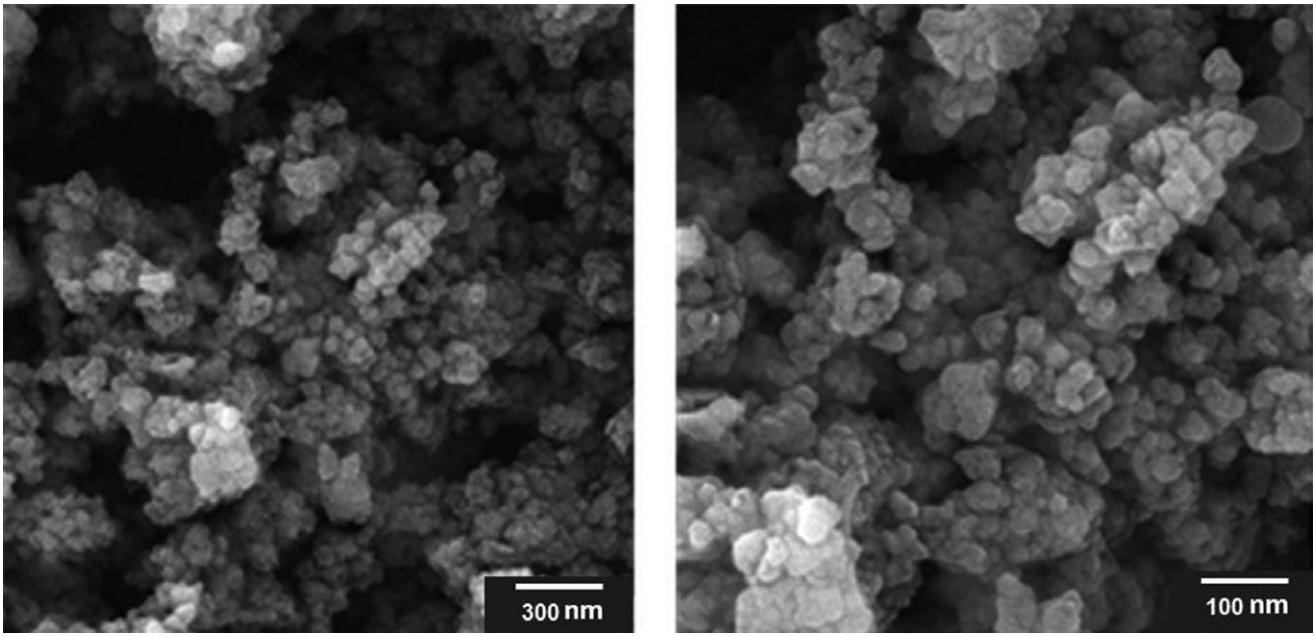

FIGURE 2 FE-SEM image of MNP–NPBG–SA nanoparticles

of C, N, Fe, O, Si, and S in the MNPs' catalyst. Thus, the presence of the S signal in the EDAX spectrum illustrates that MNP–NPBG–SA nanoparticles have been modified successfully by SO_3H groups. SEM with EDAX spectra is shown in Figure 3.

The TEM image of MNP–NPBG–SA nanocatalyst is shown (Figure 4). This study demonstrated a particle size of approximately 25 nm for the synthesized catalyst.

The crystal structure of MNP–NPBG–SA nanoparticles is evaluated using the XRD technique (Figure 5). The patterns indicate a crystallized structure at 2θ: 18.2, 30.2, 35.7, 43.2, 53.7, 57.2 and 62.7, which shows diffraction peaks, corresponding to (111), (220), (311), (400), (422), (511), and (440), respectively. According to the standard sample Fe_3O_4 (JCPDS file no. 98-007-7842), the peaks of MNPs in the XRD model is corresponded. The average crystal size of nanoparticle MNP–NPBG–SA is assessed using Debye–Scherrer's formula ($D = K\,\lambda/\beta\,\cos\,\theta$).[51] The crystal size of MNPs is about 25 nm in the range determined by FE-SEM analysis. Both the XRD patterns are colored orange for the sample of MNP–NPBG–SA that shows diffraction peaks in various angles. Figure 5 demonstrates a pattern of count peaks. According to the standard sample Fe_3O_4 (JCPDS file no. 98-007-7842) colored by blue and coesite (JCPDS file no. 98-004-5178) by green, the peaks of MNP-NPBG-SA nanoparticles in XRD model is corresponded. The elimination and addition of certain peaks because of the interaction nanoparticle is made the final factor.

Thermal gravimetric analysis (TGA) and differential thermal analysis (DTA) are used to evaluate the stability of

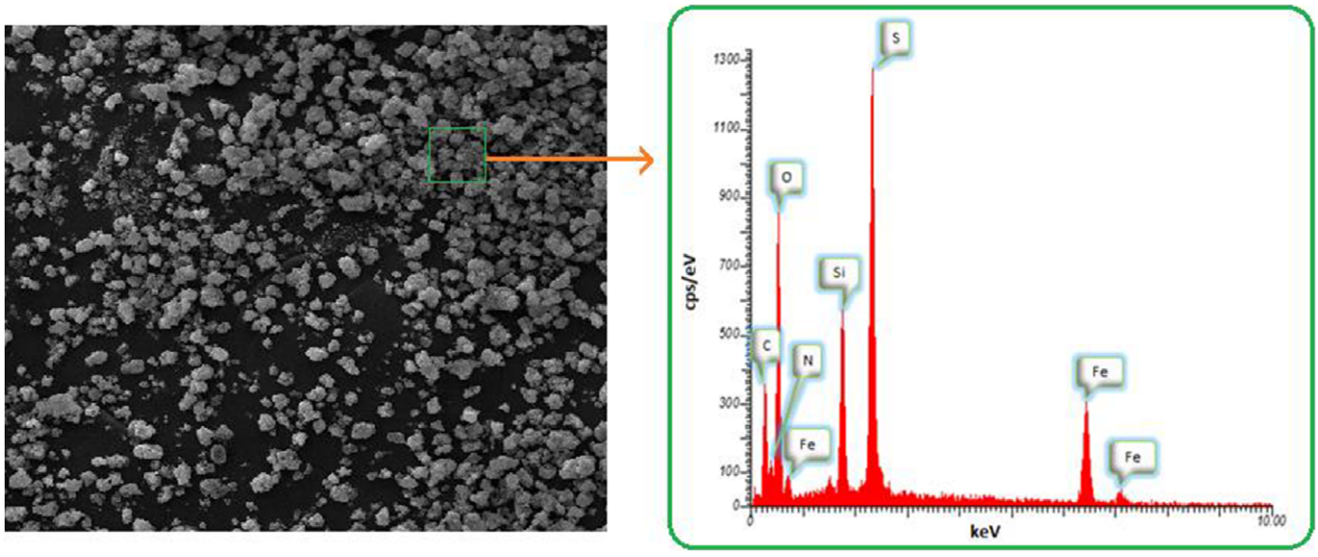

FIGURE 3 SEM with EDAX spectrum of MNP–NPBG–SA nanoparticles

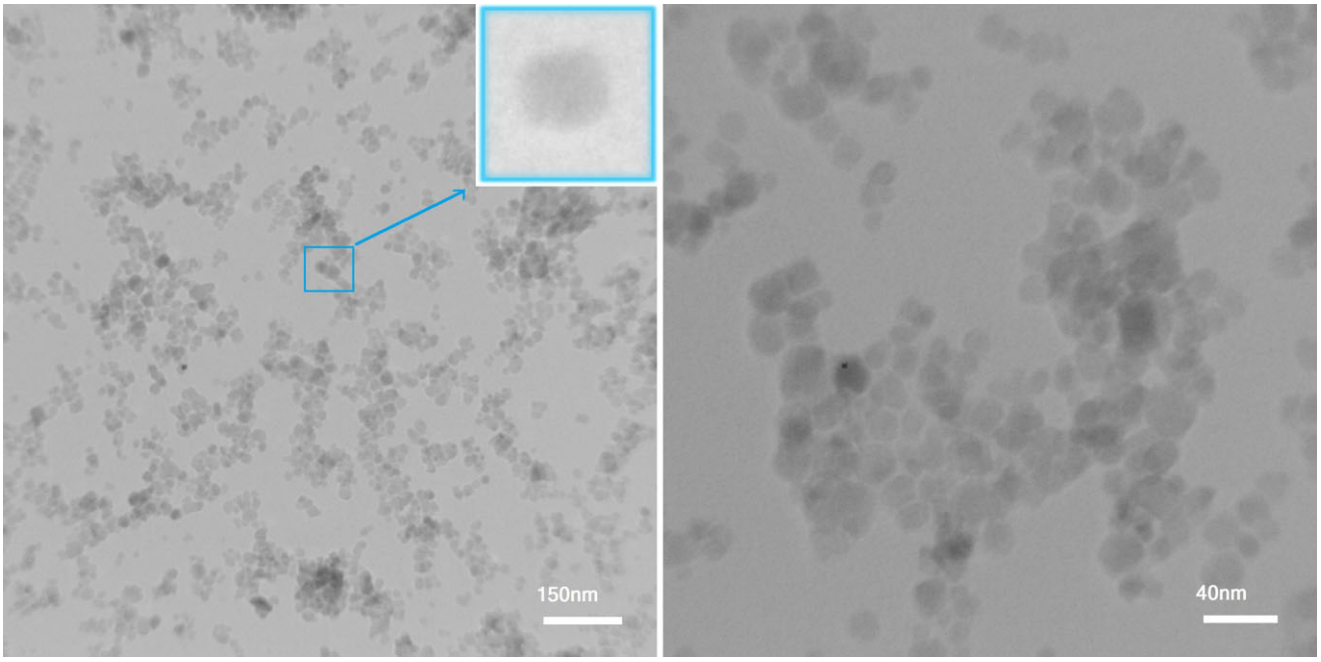

FIGURE 4 TEM images of MNP–NPBG–SA catalyst at different magnifications

MNP–NPBG–SA (Figure 6). The TGA curve shows the mass loss of MNP–NPBG–SA nanoparticles at $T < 250$ °C (10 wt%), attributed to the removal of adsorbed solvents and surface hydroxyl groups. Using DTA enabled us to find one sharp endothermic peak at 250 °C. The next stage, including the high amount of weight loss in the range of 250–600 °C, is attributed to the decomposition and evaporation of organic groups (propyl, benzoguanamine, and SO_3H) grafted to the surface of Fe_3O_4/SiO_2 MNPs.[52] Through the use of DTA, we recorded endothermic peaks at 310, 430, and 520 °C. Therefore, TGA indicated that 75% of the MNP–NPBG–SA nanoparticles consists of organic layers and 15% is Fe_3O_4/SiO_2. Thus, the MNP–NPBG–SA catalyst is stable at around 250 °C, confirming that it could be safely used in organic reactions. Thus, TGA and DTA curves also convey that the MNPs are successfully coated by organic groups.

To analyze VSM, MNP–NPBG–SA nanoparticles at a field room temperature of (±9,000 Oe) are applied (Figure 7). Magnetic saturation (Ms) for MNP–NPBG–SA nanoparticles is about 6.15 emu/g. This result shows that factorized MNPs have a low magnetic property due to the coated crust compared to the non-coated MNP (73.7 emu/g).[53] However, MNP–NPBG–SA nanoparticles can be removed from the solution using an external magnet. Thus, the strong magnetization of nanoparticles is verified due external magnetic gravity (Figure 7, left inset).

Finally, in order to quantify the amount of iron in the nanocatalyst, it was subjected to ICP-MS determination. The corresponding iron loading was found to be 1.79×10^{-4} mmol/g. In addition, to support the above observation, the sample was also analyzed through AAS and it was found that the iron content matched well with the ICP-MS result.

After the evaluation of features of the MNP–NPBG–SA nano catalyst, it was used as a heterogeneous catalyst to synthesize the new derivatives of 1,4-dihydropyridine (Scheme 1). One of the important capabilities of this nano catalyst is its novelty and ease of recovery from the reaction mixture using an external magnet, removing the necessity for filtration or centrifugation and it can be multiple times without significant performance loss.

2.2 | Synthesis of 1,4-dihydropyridines catalyzed by MNP–NPBG–SA

In order to optimize the reaction conditions, 1,4-dihydropyridine derivatives (4a, 5a) were prepared as a model compound in different amounts of catalyst, in the absence and presence of various solvents and using different temperatures, through which the reaction of barbituric acid (2 mmol), aromatic benzaldehyde (1 mmol) and ammonium acetate or aniline (1.2 mmol) was examined. The results are given in Table 1. As shown in Table 1, the best result was obtained using 7 mg of the MNP–NPBG–SA catalyst in ethanol as a safe solvent at 50 °C (Table 1, entry 9).

The conditions optimized for the production of the 1,4-dihydropyridine derivatives were evaluated using the MNP–NPBG–SA as a catalyst. The reaction of aromatic aldehydes carrying either electron-donating or electron-withdrawing substituents with barbituric acid and ammonium acetate is carried out (Table 2).

In addition, the reaction of aromatic aldehydes carrying either electron-donating or electron-withdrawing substituents with barbituric acid and aniline is carried out (Table 3). From these results, we see that all reactions proceeded smoothly to afford the corresponding products to good yields.

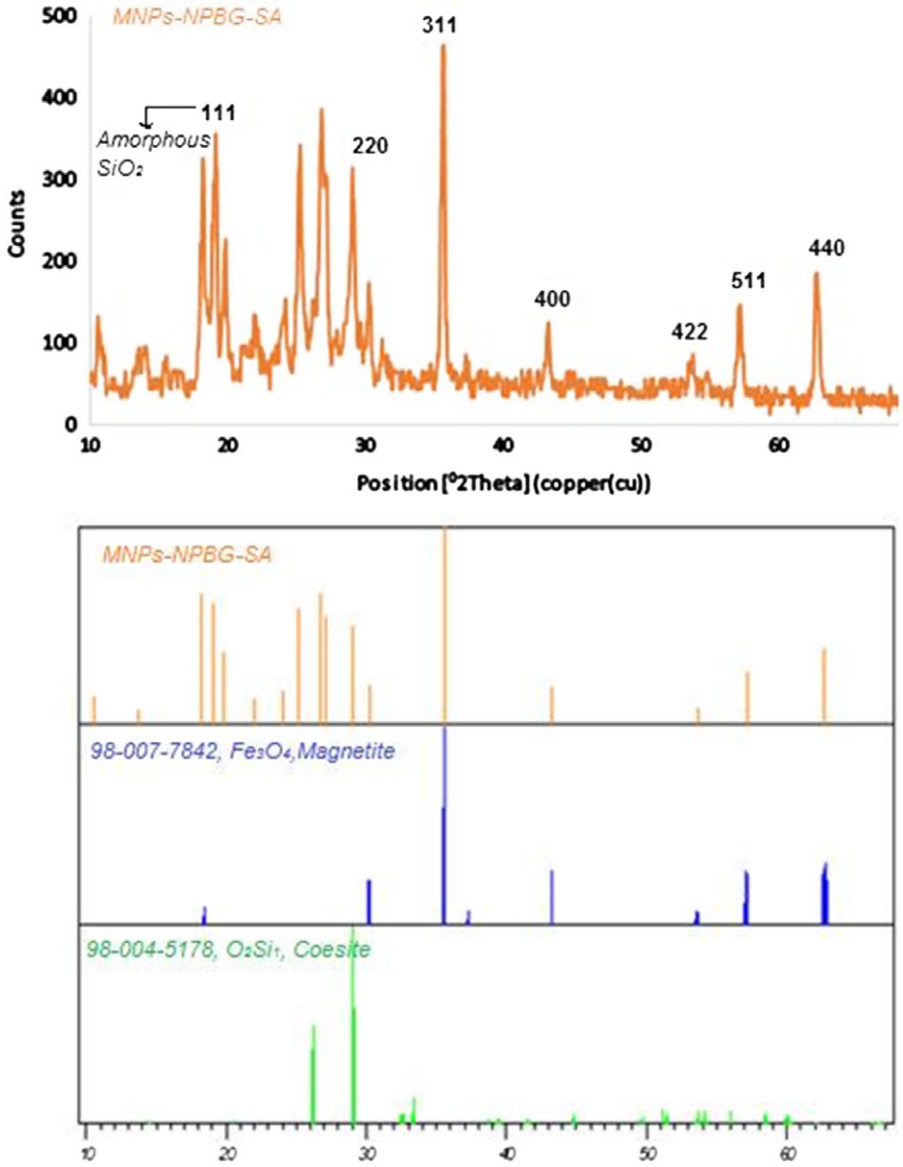

FIGURE 5 XRD diffraction pattern of MNP–NPBG–SA nanoparticles

A possible mechanism for the synthesis of 1,4-DHP in the presence of MNP–NPBG–SA as a magnetic solid acid catalyst is shown in Scheme 2. The reaction is carried out using the acidic hydrogen sulfonic acid group in the catalyst, and standard Knoevenagel condensation of aromatic aldehyde and barbituric acid takes place to form 5 as an intermediate. Then 8 attacks 5 via a Michael addition and the process continues till the target product is obtained.

2.3 | Catalyst recovery and reusability

The reusability of magnetic catalysts is one of their noteworthy advantages which, makes catalysts useful for commercial applications. In this study, the reusability of the MNP–NPBG–SA magnetic catalyst was investigated in the synthesis of the 1,4-dihydropyridine derivatives. After completion of the reaction MNP–NPBG–SA catalyst could be easily separated from the reaction mixture with the assistance of an external magnetic force and was washed with ethanol and dried at 60 °C for 1 hr. Then, the recovered catalyst was reused for the next run. The catalytic activity of MNP–NPBG–SA was examined for five runs and shows that the catalytic activity as slightly decreased because some of the MNP–NPBG–SA nanoparticles were not recovered using the external magnet or may be the result of chemical poisoning of the surface of the catalyst during the reaction (Figure 8).

After five runs, the recovered catalyst had no distinct change in structure, as shown by comparison of the FT-IR spectra with that of fresh catalyst (Figure 9).

The FE-SEM image of MNP–NPBG–SA nanoparticles after recovery after five runs is shown (Figure 10).

2.4 | Acidity of the MNP–NPBG–SA nanocatalyst

To determine the acid amount on the surface of MNPs–NPBG–SA, a back titration method was used. The MNP–

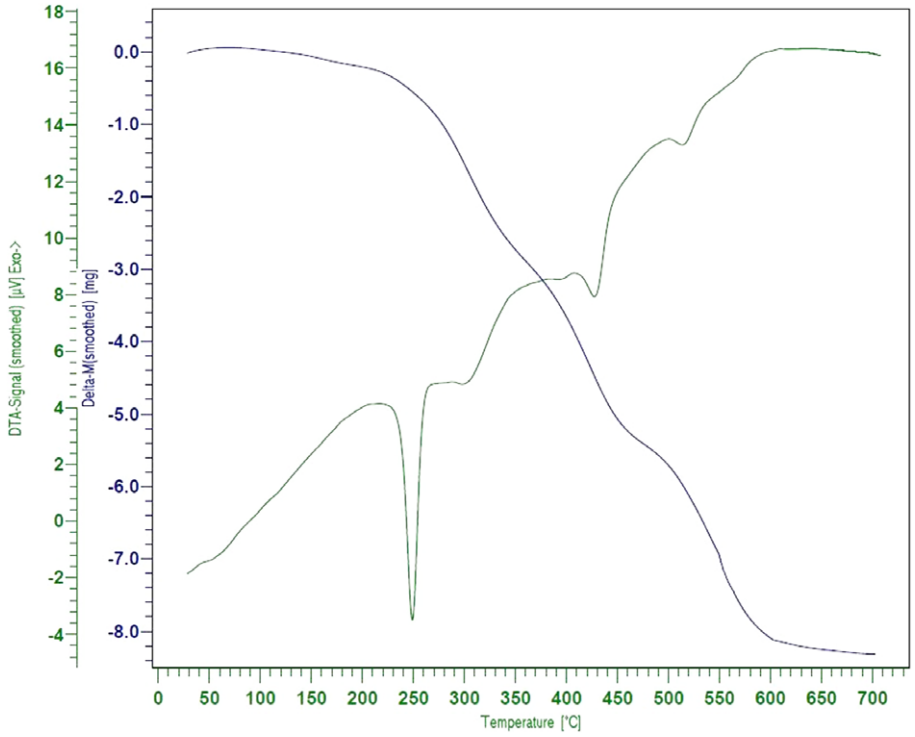

FIGURE 6 TGA/DTA analysis of MNP–NPBG–SA nanoparticles

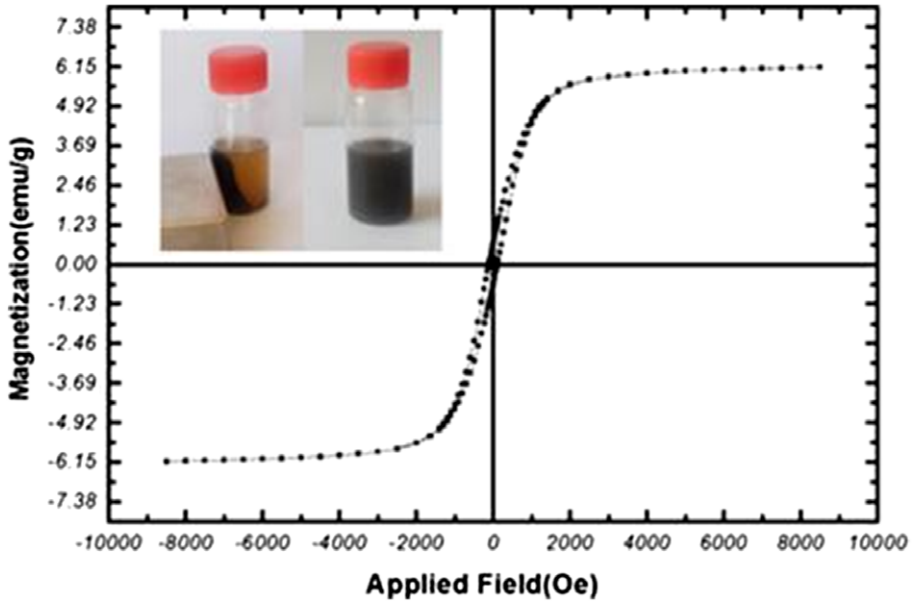

FIGURE 7 Measured magnetic hysteresis loops of the MNPs–NPBG–SA. *Left inset*: The catalyst was dispersed in liquid and captured by the external magnet

NPBG–SA nanocatalyst (0.01 g) was added to an aqueous KCl solution (1 M, 10 mL) and the resulting mixture was sonicated for 30 min, after that, the pH of the solution decreased to 2, indicating an ion exchange between nanocatalyst protons and potassium ions, the magnetic catalyst was then separated using an external magnet, and the clear solution was retained for analysis. Two drops of phenolphthalein solution were then added to the remaining solution and the resulting mixture was titrated to neutrality using a standardized 0.1 M KOH solution to determine the acid amount on the magnetic catalyst. The acid amount of the heterogeneous acidic catalyst was found to be 0.53 mmol/g.

3 | EXPERIMENTAL

3.1 | General

All chemicals were purchased from Merck or Fluka and were used without further purification. The melting points

TABLE 1 Optimization of reaction conditions for preparation of 1,4-dihydropyrirdine derivatives

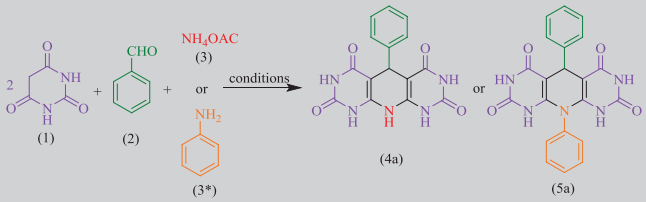

Entry	Catalyst (mg)	Solvent	Temp. (°C)	Time (min)	Yield (%)[a] 4a	Yield (%)[a] 5a
1	MNPs–NPBG–SA (3)	—	r.t.	30	23	30
2	MNPs–NPBG–SA (3)	CH_2Cl_2	r.t.	35	45	51
3	MNPs–NPBG–SA (3)	EtOH	50	45	60	58
4	MNPs–NPBG–SA (5)	H_2O	r.t.	45	74	69
5	MNPs–NPBG–SA (5)	EtOH	50	40	79	76
6	MNPs–NPBG–SA (5)	EtOH:H_2O	Reflux	15	78	80
7	MNPs–NPBG–SA (7)	EtOH	r.t.	15	70	67
8	MNPs–NPBG–SA (7)	EtOH	40	10	91	92
9	MNPs–NPBG–SA (7)	EtOH	50	10	94	95
10	MNPs–NPBG–SA (7)	EtOH	Reflux	15	90	91
11	MNPs–NPBG–SA (11)	EtOH	r.t.	20	76	78
12	MNPs–NPBG–SA (11)	EtOH	50	25	81	83
13	–	EtOH	50	60	37	39
14	MNPs–NPBG (7)	EtOH	50	40	45	50

[a] Isolated yield.

TABLE 2 Multicomponent one-pot synthesis of 1,4-dihydropyridine derivatives using MNPs–NPBG–SA as a catalyst[a]

					M.p. (°C)	
Entry	(*R*)	Product	Time (min)	Yield (%)[b]	Found	reported
1	H	**4a**	10	94	301–303	>300[36]
2	4-Me	**4b**	15	89	298–300	>300[36]
3	4-$CH(Me)_2$	**4c**	8	91	298–299[c]	—
4	3-NO_2	**4d**	15	93	297–300	>300 [36]
5	4-$N(Me)_2$	**4e**	6	90	302–304[c]	—
6	3-OH	**4f**	5	92	283–285[c]	—
7	4-F	**4g**	7	84	295–297	>300 [36]
8	4-Cl	**4h**	12	96	296–298	>300[36]
9	2-Me	**4i**	15	82	299–301[c]	—
10	3,4-$(OMe)_2$	**4j**	10	95	300–302[c]	—
11	3-OMe	**4k**	15	90	300–303	>300[36]
12	3-$CH(Me)_2$	**4l**	10	96	299–302	>300[36]
13	4-Br	**4m**	10	91	301–304	>300[36]
14	3-F	**4n**	8	87	298–301	>300[36]

[a] Aromatic aldehyde (1 mmol), barbituric acid (2 mmol), ammonium acetate (1.2 mmol) and 7 mg Fe_3O_4/SiO_2-*N*-propyl-benzoguanamine-SO_3H, at 50 °C.

[b] Isolated yield.

[c] New compound.

were uncorrected and measured using capillary tubes on an electrothermal digital apparatus. IR spectra were recorded on a Shimadzo (FT)-IR 300 spectrophotometer in KBr. ^{1}H-NMR (500 and 300 MHz), and ^{13}C-NMR spectra were obtained on Brucker 125 and 75 MHz spectrometers using $CDCl_3$ or DMSO-d_6 as a solvent with TMS as an internal standard. The progress of the reaction was monitored by thin-layer chromatography (TLC) using *n*-hexane/EtOAc as an eluent. Nanoparticles were characterized using an X-Pert Pro MPD XRD diffractometer (Cu-K_α, k = 0.154056 nm) over the range 2θ = 10–80 using 0.04° as the step length. The scanning electron microscope measurement was

TABLE 3 Multicomponent one-pot synthesis of 1,4-dihydropyridine derivatives using MNPs–NPBG–SA as a catalyst[a]

Entry	(*R*)	Product	Time (min)	Yield (%)[a]	M.p. (°C) Found reported	
1	H	**5a**	10	94	204–206[c]	—
2	4-Me	**5b**	5	85	158–160[c]	—
3	4-$CH(Me)_2$	**5c**	7	90	192–194[c]	—
4	3-NO_2	**5d**	5	91	210–212[c]	—
5	4-$N(Me)_2$	**5e**	5	88	284–286[c]	—
6	3-OH	**5f**	6	93	206–208[c]	—
7	4-NO_2	**5g**	10	94	205–207[c]	—
8	4-Cl	**5h**	6	90	198–200[c]	—
9	2-Me	**5i**	15	89	245–247[c]	—
10	3,4-$(OMe)_2$	**5j**	9	94	280–282[c]	—

[a] Isolated yield.

[b] Aromatic aldehyde (1 mmol), barbituric acid (2 mmol), aniline (1.2 mmol) and 7 mg Fe_3O_4/SiO_2-*N*-propyl-benzoguanamine-SO_3H, at 50 °C.

[c] New compound.

obtained using a Hitachi S-4700 field emission-scanning electron microscope (FE-SEM). TEM analysis of the catalyst was recorded using Zeiss-EM10C TEM. The thermogravimetric analysis (TGA) and DTA curves were recorded using Diamond TGA/DTA SII of the Perkin Elmer Company. The magnetization was measured at room temperature using a vibrating sample magnetometer (Model 7300 VSM System, Lake Shore Cryotronic, Inc., Westerville, OH). ICP-MS was also performed in order to confirm the iron-loading ICP-MS (Model Elan 6,000 DRC). The iron content in the catalyst supernatant was estimated through atomic absorption spectroscopy (AAS) on a Model novAA-400p atomic absorption spectrometer.

3.2 | General procedure for preparation of MNP–NPBG–SA

Fe_3O_4 MNPs were prepared by chemical co-precipitation of Fe^{3+} and Fe^{2+} ions as described in the literature.[54] The Fe_3O_4 coated with SiO_2 was prepared through a modified sol–gel method.[55] Chloropropyl-modified silica-coated MNPs were prepared according to a reported procedure.[56] To a magnetically stirred mixture of the prepared Fe_3O_4/SiO_2-Chloropropyl (1 g) was added benzoguanamine (10 mmol, 1.87 g) and triethylamine (10 mmol, 1.39 mL) in dried toluene (50 mL) and the mixture was sonicated for 2 hr under N_2 atmosphere and then stirred for 48 hr under reflux conditions. The obtained solid was magnetically collected from the solution and washed with water/ethanol (20:10 mL) thrice and dried in vacuum for 5 hr. To a mixture of benzoguanamine-modified silica-coated Fe_3O_4 MNPs (1 g) in dried $CHCl_3$ (3 mL), chlorosulfonic acid ($ClSO_3H$, 1 mL) was added dropwise at 0 °C over 2 hr and then the mixture was filtered and washed with ethanol (5 mL) and dried at room temperature to afford the title compound. MNP–NPBG–SA particles were prepared via the procedure illustrated in Scheme 3.

3.3 | General procedure for synthesis of 1, 4-DHP derivatives

The mixture of barbituric acid (2 mmol), aromatic benzaldehyde (1 mmol), and ammonium acetate or aniline (1.2 mmol) was added to MNPs–NPBG–SA (7 mg) in 5 mL of ethanol as the solvent and the reaction mixture was stirred magnetically at 50 °C. The progress of the reaction was followed by TLC. After the completion of the reaction, the mixture was cooled to room temperature, and the catalyst was easily separated by an external magnet. The solvent was evaporated to afford the crude solid. Finally, the resulting solid was filtered and then washed with ethanol without further purification and dried in an oven at 60 °C. The pure 1,4-dihydropyridine derivatives were obtained in excellent yields.

4 | SELECTED SPECTRAL DATA

4.1 | 5-phenyl-5,10-dihydropyrido[2,3-d:6,5-d′] dipyrimidine-2,4,6,8(1H,3H,7H,9H)-tetraone (4a)

White solid; m.p: 301–303 °C; Yield 94%; ^{1}H NMR (500 MHz, DMSO-d_6) δppm: 5.90 (s, 1H, CH), 7.01–7.11 (m, 5H, Ar-H), 7.12 (s, 1H, NH $_{1,4\text{-dihydropyridine}}$), and 10.15 (s, 4H, NH); ^{13}C NMR (125 MHz, DMSO-d_6) δppm: 31.3, 91.9, 125.3, 127.5, 128.3, 145.4, 151.6, and 166.8.

4.2 | 5-(p-tolyl)-5,10-dihydropyrido[2,3-d:6,5-d′] dipyrimidine-2,4,6,8(1H,3H,7H,9H)-tetraone (4b)

White solid; m.p: 298–300 °C; Yield 89%; ^{1}H NMR (500 MHz, DMSO-d_6) δppm: 2.16 (s, 3H, CH_3), 5.84 (s, 1H, CH), 6.84–6.86 (d, 2H, Ar-H, J = 7.95 Hz), 6.89–6.90 (d, 2H, Ar-H, J = 8.05 Hz), 7.07 (s, 1H, $NH_{1,4\text{-dihydropyridine}}$, D_2O-exchangable), 10.0 (s, 4H, NH, D_2O-exchangable); ^{13}C NMR (125 MHz, DMSO-d_6) δppm: 21.4, 30.9, 92.0, 127.5, 128.9, 133.9, 142.4, 151.6.

4.3 | 5-(3-nitrophenyl)-5,10-dihydropyrido [2,3-d:6,5-d′]dipyrimidine-2,4,6,8(1H,3H,7H,9H)-tetraone (4d)

White solid; m.p: 297–300 °C; Yield 93%; ^{1}H NMR (500 MHz, DMSO-d_6) δppm: 6.04 (s, 1H, CH), 7.03 (s, 1H, NH $_{1,4\text{-dihydropyridine}}$), 7.41–7.46 (m, 2H, Ar-H), 7.80 (s, 1H, Ar-H), 7.88–7.89 (d, 1H, Ar-H, J = 1.5 Hz), and 9.98 (s, 4H, NH); ^{13}C NMR (125 MHz, DMSO-d_6) δppm: 31.7, 91.1, 120.6, 121.9, 129.7, 134.6, 148.5, 148.9, 151.5, and 165.6.

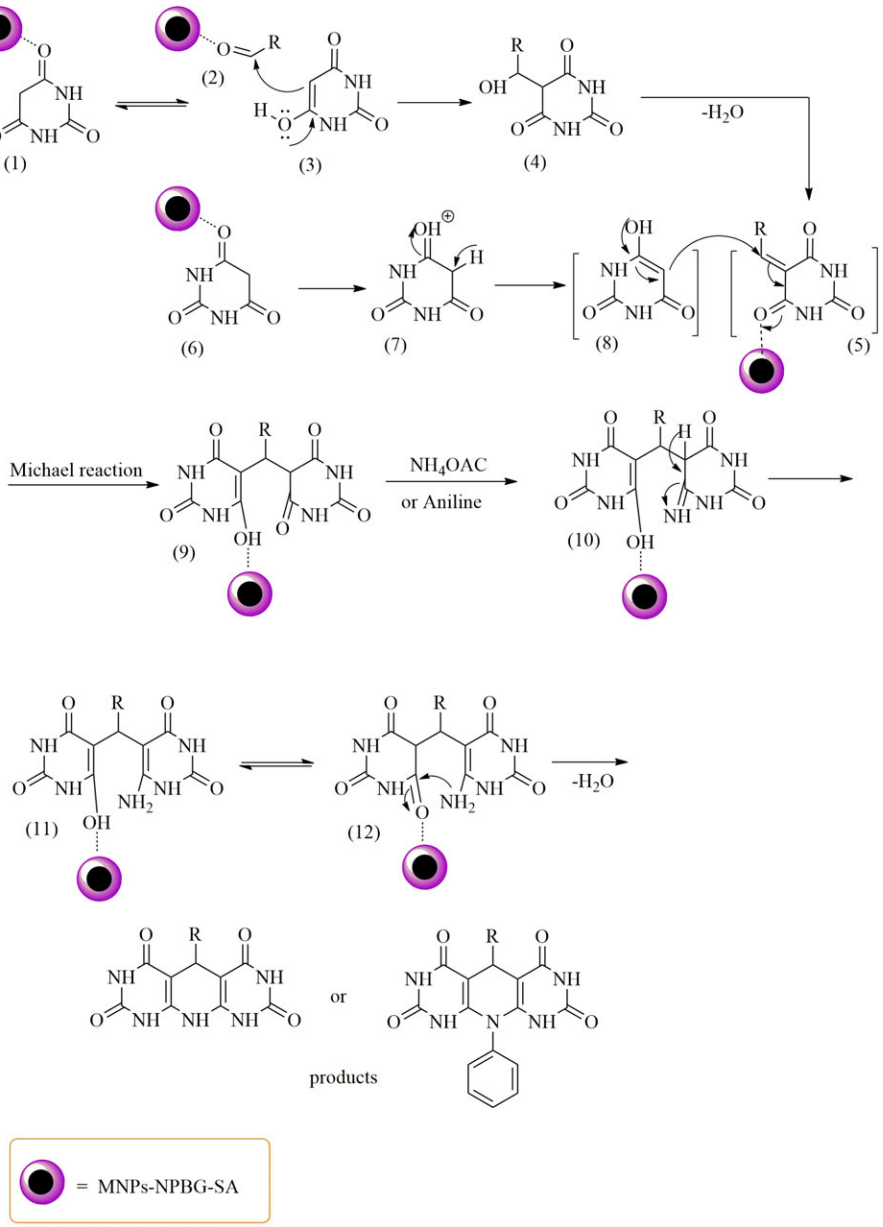

SCHEME 2 Proposed mechanism for synthesis of 1,4-DHP using MNPs–NPBG–SA as catalyst

4.4 | 5-(4-fluorophenyl)-5,10-dihydropyrido [2,3-d:6,5-d′]dipyrimidine-2,4,6,8(1H,3H,7H,9H)-tetraone (4g)

White solid; m.p: 295–297 °C; Yield 84%; ^{1}H NMR (500 MHz, DMSO-d_6) δppm: 5.87 (s, 1H, CH), 6.89–6.91 (d, 2H, Ar-H, J = 10.0 Hz), 6.99–7.02 (d, 2H, Ar-H, J = 10.0 Hz), 7.09 (s, 1H, NH $_{1,4\text{-dihydropyridine}}$), and 10.05 (s, 4H, NH); ^{13}C NMR (125 MHz, DMSO-d_6) δppm: 30.8, 91.8, 114.7, 114.8, 129.09, 129.1, 141.5, 151.5, 159.8, and 161.7.

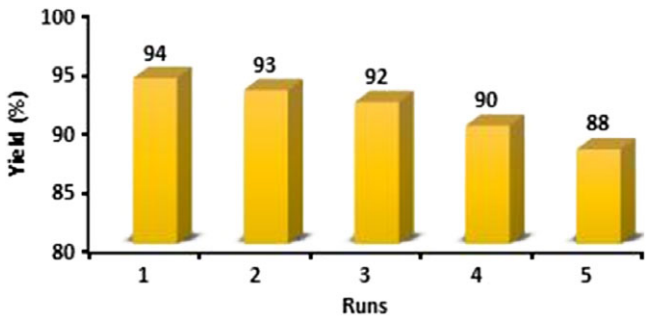

FIGURE 8 Recyclability of MNPs–NPBG–SA in the synthesis of 1,4-DHP derivatives

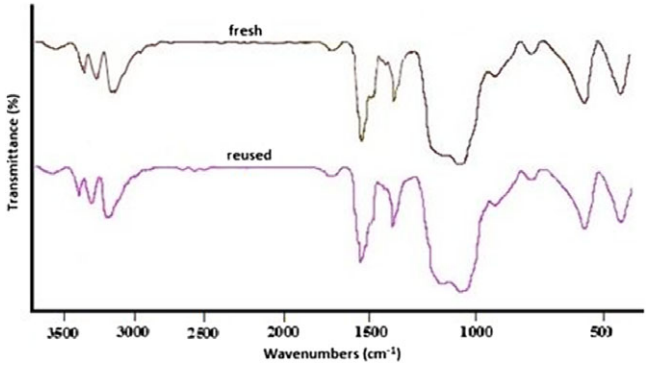

FIGURE 9 FT-IR spectra of fresh catalyst and a catalyst that has been reused five times

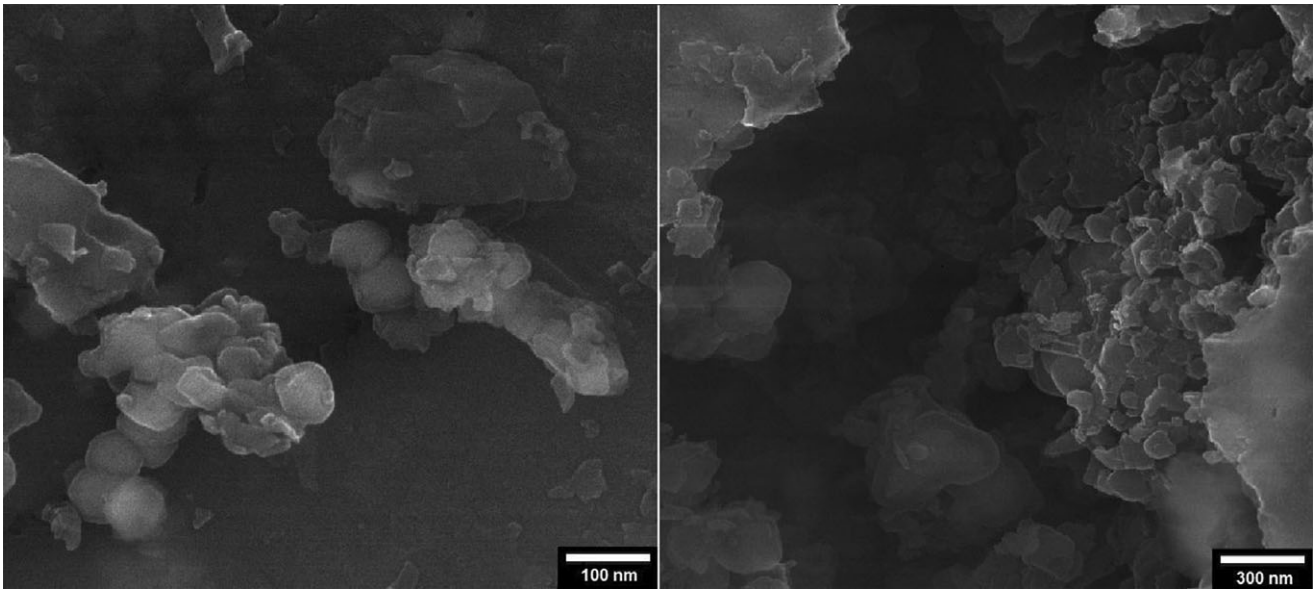

FIGURE 10 FE-SEM image of MNP–NPBG–SA nanoparticles after recovery after five runs

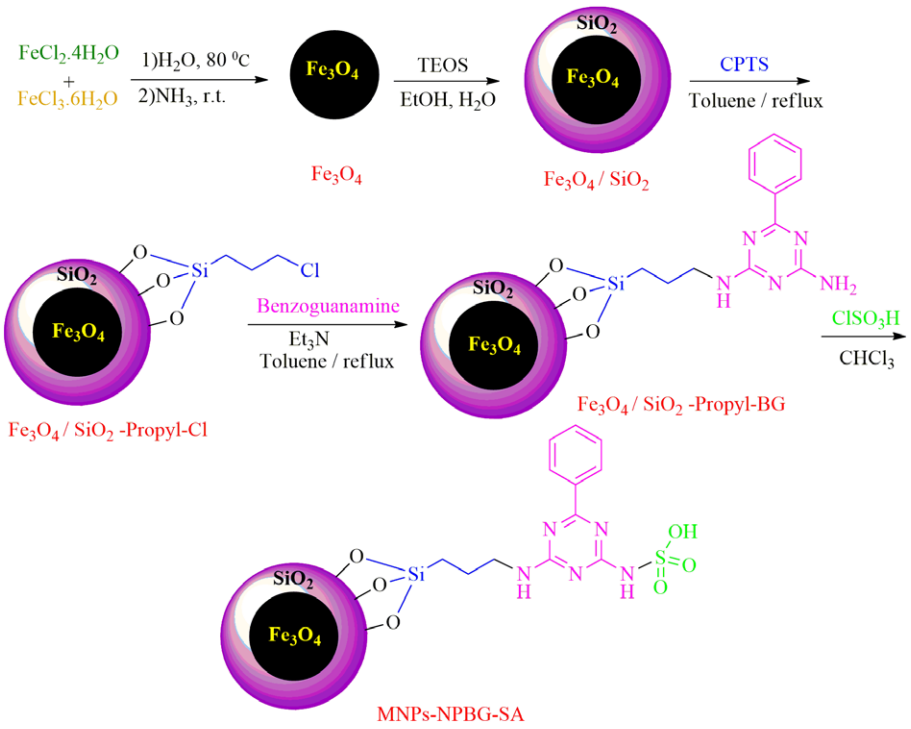

SCHEME 3 Preparation of *N*-propylbenzoguanamine sulfonic acid stabilized on silica-coated nano-Fe_3O_4 particles (MNP–NPBG–SA)

4.5 | 5-(4-chlorophenyl)-5,10-dihydropyrido [2,3-d:6,5-d′]dipyrimidine-2,4,6,8(1H,3H,7H,9H)-tetraone (4h)

White solid; m.p: 296–298 °C; Yield 96%; ^{1}H NMR (500 MHz, $CDCl_3$) δppm: 5.92 (s, 1H, CH), 7.01–7.03 (d, 2H, Ar-H, J = 8.0 Hz), 7.11 (s, 1H, $NH_{1,4\text{-dihydropyridine}}$), 7.18–7.20 (d, 2H, Ar-H, J = 8.0 Hz), and 10.09 (s, 4H, NH); ^{13}C NMR (125 MHz, $CDCl_3$) δppm: 31.0, 91.6, 128.1, 129.4, 129.7, 144.8, and 151.5.

4.6 | 5-(3-isopropylphenyl)-5,10-dihydropyrido [2,3-d:6,5-d′]dipyrimidine-2,4,6,8(1H,3H,7H,9H)-tetraone (4l)

White solid; m.p: 299–302 °C; Yield 96%; ^{1}H NMR (500 MHz, DMSO-d_6) δppm: 1.15 (s, 3H, CH_3), 1.17 (s, 3H, CH_3), 2.50–2.81 (m, 1H, CH), 5.90 (s, 1H, CH), 6.92–7.01 (m, 4H, Ar-H), 7.11 (s, 1H, $NH_{1,4\text{-dihydropyridine}}$), and 10.0 (s, 4H, NH); ^{13}C NMR (125 MHz, DMSO-d_6) δppm: 24.3, 24.4, 24.9, 30.9,

33.7, 34.5, 91.9, 126.1, 127.4, 128.0, 129.0, 130.6, 142.9, 145.1, 151.6, and 164.8.

4.7 | 5-(4-bromophenyl)-5,10-dihydropyrido [2,3-d:6,5-d′]dipyrimidine-2,4,6,8(1H,3H,7H,9H)-tetraone (4m)

White solid; m.p: 301–304 °C; Yield 91%; ^{1}H NMR (500 MHz, DMSO-d_6) δppm: 5.85 (s, 1H, CH), 6.92–6.94 (d, 2H, Ar-H, J = 8.2 Hz), 7.06 (s, 1H,, $NH_{1,4\text{-dihydropyridine}}$), 7.27–7.29 (d, 2H, Ar-H, J = 8.4 Hz), and 10.09 (s, 4H, NH); ^{13}C NMR (125 MHz, DMSO-d_6) δppm: 31.3, 91.5, 118.2, 129.9, 131.1, 145.2, and 151.6.

4.8 | 5,10-diphenyl-5,10-dihydropyrido[2,3-d:6,5-d′] dipyrimidine-2,4,6,8(1H,3H,7H,9H)-tetraone (5a)

White solid; m.p: 204–206 °C; Yield 95%; IR (KBr, cm^{-1}) ν_{max}: 1,696 (C=O), 3,129 and 3,339 (NH); ^{1}H-NMR (DMSO-d_6, 300 MHz) δppm: 5.92 (s, 1H, CH), 7.02–7.48 (m, 5H, Ar-H, $_{symmetric}$), 10.2 (brs, 1H, NH, $_{symmetric}$), and 11.12 (brs, 1H, NH, $_{symmetric}$); ^{13}C-NMR (DMSO-d_6, 75 MHz) δppm: 30.8, 67.8, 84.8, 91.1, 120.4, 124.7, 126.7, 127.4, 129.5, 136.8, 150.7, and 164.8.

4.9 | 10-phenyl-5-(p-tolyl)-5,10-dihydropyrido [2,3-d:6,5-d′]dipyrimidine-2,4,6,8(1H,3H,7H,9H)-tetraone (5b)

White solid; m.p: 158–160 °C; Yield 85%; IR (KBr, cm^{-1}) ν_{max}: 1,691 (C=O), 3,139 and 3,182 (NH); ^{1}H-NMR (DMSO-d_6, 300 MHz) δppm: 2.2 (s, 3H, CH_3), 5.9 (s, 1H, CH), 6.94–7.25 (m, 9H, 2 Ar-H), 10.14 (brs, 2H, NH), 11.16 (brs, 2H, NH); ^{13}C-NMR (DMSO-d_6, 75 MHz) δppm: 20.6, 30.3, 61.6, 68.4, 119.2, 122.8, 126.7, 128.1, 128.6, 128.8, 129.4, 129.7, 133.2, 139.2, 140.9, 150.8, 169.6.

4.10 | 5-(4-isopropylphenyl)-10-phenyl-5,10-dihydropyrido[2,3-d:6,5-d′]dipyrimidine-2,4,6,8 (1H,3H,7H,9H)-tetraone (5c)

Yellow solid; m.p: 192–194 °C; Yield 90%; IR (KBr, cm^{-1}) ν_{max}: 1,689 (C=O), 3,140 and 3,408 (NH); ^{1}H-NMR (DMSO-d_6, 300 MHz) δppm: 1.13 (s, 3H, CH_3), 1.15 (s, 3H, CH_3), 2.77–2.79 (m, 1H, CH), 5.87 (s, 1H, CH), 7.08–7.09 (m, 5H, Ar-H), 7.28–7.32 (dd, 4H, Ar-H, J = 7.2 Hz), 10.20 (brs, 2H, NH), and 11.20 (brs, 2H, NH); ^{13}C-NMR (DMSO-d_6, 75 MHz) δppm: 23.7, 24.1, 32.6, 73.9, 87.7, 91.0, 120.1, 123.9, 125.3, 126.6, 129.4, 137.3, 150.6, 163.7, and 165.9.

4.11 | 5-(3-nitrophenyl)-10-phenyl-5,10-dihydropyrido [2,3-d:6,5-d′]dipyrimidine-2,4,6,8(1H,3H,7H,9H)-tetraone (5d)

White solid; m.p: 210–212 °C; Yield 91%; IR (KBr, cm^{-1}) ν_{max}: 1,301 and 1,525 (NO_2), 1,690 (C=O), 3,126 and 3,407 (NH); ^{1}H-NMR (DMSO-d_6, 500 MHz) δppm: 6.05 (s, 1H, CH), 7.18–7.37 (m, 5H, Ar-H), 7.47–7.82 (m, 3H, Ar-H), 7.93 (s, 1H, Ar-H), and 10.21 (brs, 4H, NH); ^{13}C-NMR (DMSO-d_6, 125 MHz) δppm: 30.9, 90.03, 119.9, 120.9, 121.05, 125.1, 128.9, 129.5, 133.8, 135.8, 147.5, 147.7, 150.5, 164.8, 167.7, and 168.6.

4.12 | 5-(4-[dimethylamino]phenyl)-10-phenyl-5,10-dihydropyrido[2,3-d:6,5-d′]dipyrimidine-2,4,6,8 (1H,3H,7H,9H)-tetraone (5e)

White solid; m.p: 284–286 °C; Yield 88%; IR (KBr, cm^{-1}) ν_{max}: 1,657 and 1,721 (C=O),2,817–2,927 (CH_3 str.), 3,071 and 3,192 (NH); ^{1}H-NMR (DMSO-d_6, 300 MHz) δppm: 3.09 (s, 6H, $2CH_3$), 6.74 (s, 1H, CH), 8.12–8.40 (m, 9H, 2Ar-H), 10.9 (s, 2H, NH), and 11.03 (s, 2H, NH); ^{13}C-NMR (DMSO-d_6, 75 MHz) δppm: 33.03, 57.6, 73.6, 90.9, 99.3, 104.7, 109.5, 111.2, 120.0, 139.1, 141.7, 150.3, 154.1, 155.5, 162.7, and 164.7.

4.13 | 5-(3-hydroxyphenyl)-10-phenyl-5,10-dihydropyrido[2,3-d:6,5-d′]dipyrimidine-2,4,6,8 (1H,3H,7H,9H)-tetraone (5f)

White solid; m.p: 206–208 °C; Yield 93%; IR (KBr, cm^{-1}) ν_{max}: 1,690 (C=O), 3,126 and 3,343 (NH), 3,407 (OH); ^{1}H-NMR (DMSO-d_6, 500 MHz) δppm: 5.83 (s, 1H, CH), 6.41–7.00 (m, 5H, Ar-H), 7.27–7.62 (m, 4H, Ar-H), 10.12 (brs, 4H, NH), and 11.17 (s, 1H, OH); ^{13}C-NMR (DMSO-d_6, 125 MHz) δppm: 30.7, 91.1, 111.5, 113.9, 117.6, 119.8, 123.5, 128.2, 129.4, 138.1, 146.0, 150.7, 151.8, 156.8, 164.1, 165.8, and 167.8.

4.14 | 5-(4-nitrophenyl)-10-phenyl-5,10-dihydropyrido [2,3-d:6,5-d′]dipyrimidine-2,4,6,8(1H,3H,7H,9H)-tetraone (5g)

White solid; m.p: 205–207 °C; Yield 94%; IR (KBr, cm^{-1}) ν_{max}: 1,346 and 1,509 (NO_2), 1,714 (C=O), 3,149 and 3,400 (NH); ^{1}H-NMR (DMSO-d_6, 300 MHz) δppm: 6.06 (s, 1H, CH), 7.29–7.39 (m, 9H, 2Ar-H), and 10.34 (brs, 4H, NH); ^{13}C-NMR (DMSO-d_6, 75 MHz) δppm: 31.5, 56.2, 90.5, 104.9, 122.2, 122.9, 126.7, 127.9, 129.7, 133.8, 137.3, 145.0, 150.8, 153.9, 155.3, 158.7, 159.4, and 165.0.

4.15 | 5-(4-chlorophenyl)-10-phenyl-5,10-dihydropyrido[2,3-d:6,5-d′]dipyrimidine-2,4,6,8 (1H,3H,7H,9H)-tetraone (5h)

Yellow solid; m.p: 198–200 °C; Yield 90%; IR (KBr, cm^{-1}) ν_{max}: 686–838 (Cl), 1,689 (C=O), 3,146 and 3,400 (NH); ^{1}H-NMR (DMSO-d_6, 500 MHz) δppm: 5.88 (s, 1H, CH), 7.03–7.51 (m, 9H, 2Ar-H), and 10.15 (brs, 4H, NH); ^{13}C-NMR (DMSO-d_6, 75 MHz) δppm: 30.5, 56.1, 76.0, 90.6, 106.1, 121.7, 126.1, 127.4, 128.6, 129.1, 129.7, 134.7, 143.4, 150.7, and 163.8.

4.16 | 10-phenyl-5-(o-tolyl)-5,10-dihydropyrido [2,3-d:6,5-d′]dipyrimidine-2,4,6,8(1H,3H,7H,9H)-tetraone (5i)

Yellow solid; m.p: 245–247 °C; Yield 89%; IR (KBr, cm^{-1}) ν_{max}: 1,690 (C=O), 2,825–2,852 (CH_3, str.), 3,060 and 3,123 (NH); ^{1}H-NMR (DMSO-d_6, 500 MHz) δppm: 3.48 (s, 3H, CH_3), 4.96 (brs, 1H, CH), 6.48–6.99 (m, 9H, 2Ar-H), and 11.1 (s, 4H, NH); ^{13}C-NMR (DMSO-d_6, 75 MHz) δppm: 20.6, 30.3, 61.6, 68.4, 119.2, 122.8, 126.7, 128.1, 128.6, 128.8, 129.4, 129.7, 133.2, 139.2, 140.9, 150.8, and 169.6.

4.17 | 5-(3,4-dimethoxyphenyl)-10-phenyl-5,10-dihydropyrido[2,3-d:6,5-d′]dipyrimidine-2,4,6,8 (1H,3H,7H,9H)-tetraone (5j)

White solid; m.p: 280–282 °C; Yield 94%; IR (KBr, cm^{-1}) ν_{max}: 1,150–1,389 (OCH_3), 1,741 (C=O), 3,136 and 3,224 (NH); ^{1}H-NMR (DMSO-d_6, 300 MHz) δppm: 3.79 (s, 3H, OCH_3), 3.86 (s, 3H, OCH_3), 7.08 (s, 1H, CH), 7.39–7.84 (m, 8H, 2 Ar-H), 11.16 (s, 2H, NH), and 11.3 (s, 2H, NH); ^{13}C-NMR (DMSO-d_6, 75 MHz) δppm: 30.08, 55.5, 55.9, 81.1, 111.1, 115.2, 116.8, 125.3, 131.8, 147.8, 150.2, 153.7, 155.5, 162.4, and 164.0.

5 | CONCLUSIONS

We have developed a simple and highly efficient protocol for the synthesis of new derivatives of 1,4-dihydropyridine through the one-pot pseudo-four-component condensation of barbituric acid, aromatic aldehydes, and ammonium acetate or aniline with *N*-propylbenzoguanamine sulfonic acid, stabilized on silica-coated nano-Fe_3O_4 particles (MNP–NPBG–SA) as a new and reusable heterogeneous catalyst in ethanol at 50 °C. The process offers several advantages, including a green solvent system; mild reaction conditions; use of easily available, cheap, high yields; shorter reaction time and easy workup; and reusability of the catalyst. The MNP–NPBG–SA nanocatalyst was characterized using FT-IR spectroscopy, XRD, FE-SEM, EDAX, TEM, VSM, TGA, DTA, ICP-MS, and AAS.

ACKNOWLEDGMENTS

We gratefully acknowledge the financial support from the Research Council of Aja University of Medical Sciences and Islamic Azad University-Tehran North Branch.

ORCID

Naser Foroughifar http://orcid.org/0000-0003-0562-3015

REFERENCES

[1] (a) G. K. S. Prakash, H. Lau, C. Panja, I. Bychinskaya, S. K. Ganesh, B. Zaro, T. Mathew, G. A. Olah, *Catal. Lett.* **2014**, *144*, 2012. (b) L. Han, H. J. Choi, S. J. Choi, B. Liub, D. W. Park, *Green Chem.* **2011**, *13*, 1023.
[2] (a) L. Han, S. W. Park, D. W. Park, *Energy Environ. Sci.* **2009**, *2*, 1286. (b) G. Rahimzadeh, S. Bahadorikhalili, E. Kianmehr, M. Mahdavi, *Mol. Divers.* **2017**, *21*, 597.
[3] S. R. Jagtap, V. P. Raje, S. D. Samant, B. M. Bhanage, *J. Mol. Catal. A* **2007**, *266*, 69.
[4] J. Sun, S. Fujita, F. Zhao, M. Araj, *Green Chem.* **2004**, *6*, 613.
[5] A. Corma, H. Garcia, *Adv. Synth. Catal.* **2006**, *348*, 1391.
[6] (a) M. Shah Hosseini, H. Ghafuri, H. R. Esmaili Zand, *J. Chin. Chem. Soc.* **2018**, *1*. https://doi.org/10.1002/jccs.201700455.(b) L. Shiri, A. Ghorbani-Choghamarani, M. Kazemi, *Res. Chem. Intermed.* **2017**, *43*, 2707.
[7] A. Kiasat, J. Davarpanah, *Res. Chem. Intermed.* **2015**, *41*, 2991.
[8] (a) P. Zhang, M. Shi, M. Fan, P. Jiang, Y. Dong, *J. Chin. Chem. Soc.* **2018**, *65*. https://doi.org/10.1002/jccs.201700368.(b) S. Kangari, I. Yavari, *Res. Chem. Intermed.* **2016**, *42*, 8217.
[9] M. Samadizadeh, S. Nouri, F. Kiani Moghadam, *Res. Chem. Intermed.* **2016**, *42*, 6089.
[10] R. B. N. Baig, R. S. Varma, *Chem. Commun.* **2013**, *49*, 752.
[11] T. Sen, A. Sebastianelli, I. J. Bruce, *J Am. Chem. Soc.* **2006**, *128*, 7130.
[12] R. S. Chaughule, S. Purushotham, R. V. Ramanujan, *Proc. Natl. Acad. Sci. India Sect. A Phys. Sci.* **2012**, *82*, 257.
[13] T. Neuberger, B. Schöpf, H. Hofmann, M. Hofmann, B. V. Rechenberg, *J Magn. Magn. Mater.* **2005**, *293*, 483.
[14] H. Gu, K. Xu, C. Xu, B. Xu, *Chem. Commun.* **2006**, *9*, 941.
[15] I. Akira, T. Kouji, K. Kazuyoshi, S. Masashige, H. Hiroyuki, M. Kazuhiko, S. Toshiaki, K. Takeshi, *Cancer Sci.* **2003**, *94*, 308.
[16] S. Bahceci, B. Unal, A. Baykal, H. Sozerid, E. Karaoglua, B. Esata, *J Alloys Compd.* **2011**, *509*, 8825.
[17] W. Wu, Q. He, C. Jiang, *Nanoscale Res. Lett.* **2008**, *3*, 397.
[18] (a) K. Singh, A. Ohlan, A. K. Bakhshia, S. K. Dhawan, *Mater. Chem. Phys.* **2010**, *119*, 201. (b) M. Aydin, Z. Durmus, H. Kavas, B. Esat, H. Sözeri, A. Baykal, F. Yılmaz, M. S. Toprak, *Polyhedron* **2011**, *30*, 1120.
[19] Y. Li, G. Chen, Q. Li, G. Qiu, X. Liu, *J. Alloys Compd.* **2011**, *509*, 4104.
[20] A. Maleki, Z. Alrezvani, S. Maleki, *Catal. Comm.* **2015**, *69*, 29.
[21] Y. H. Leng, K. Sato, Y. G. Shi, J. G. Li, T. Ishigaki, T. Yoshida, H. Kamiya, *J Phys. Chem. C* **2009**, *113*, 16681.
[22] A. L. Morel, S. I. Nikitenko, K. Gionnet, A. Wattiaux, J. Lai-Kee-Him, C. Labrugere, B. Chevalier, G. Deleris, C. Petibois, A. Brisson, M. Simonoff, *ACS Nano* **2008**, *2*, 847.
[23] H.-Y. Lian, M. Hu, C.-H. Liu, Y. Yamauchi, K. C.-W. Wu, *Chem. Commun.* **2012**, *48*, 5151.
[24] F.-K. Shieh, S.-C. Wang, C.-I. Yen, C.-C. Wu, S. Dutta, L.-Y. Chou, J. V. Morabito, P. Hu, M.-H. Hsu, K. C.-W. Wu, C.-K. Tsung, *JACS* **2015**, *137*, 4276.
[25] K. C.-W. Wuab, Y. Yamauchi, *J. Mater. Chem.* **2012**, *22*, 1251.
[26] J. L. Vivero-Escoto, Y.-D. Chiang, K. C.-W. Wu, Y. Yamauchi, *Sci. Technol. Adv. Mater.* **2012**, *13*, 013003.
[27] K. C.-W. Wu, Y. Yamauchi, C.-Y. Hong, Y.-H. Yang, Y.-H. Liang, T. Funatsud, M. Tsunodad, *Chem. Commun.* **2011**, *47*, 5232.
[28] (a) J. Zhu, H. Bienayme, *Multicomponent Reactions*, Wiley-VCH, Weinheim **2005**. (b) A. Domling, I. Ugi, *Angew. Chem. Int. Ed.* **2000**, *39*, 3168.
[29] C. Simon, T. Constantieux, J. Rodriguez, *Eur. J. Org. Chem.* **2004**, *2004*, 4957.
[30] L.-M. Wang, J. Sheng, L. Zhang, J.-W. Han, Z. Fan, H. Tian, C.-T. Qian, *Tetrahedron* **2005**, *6*, 1539.
[31] T. R. Ravikumar Naik, S. A. Shivashankar, *Tetrahedron Lett.* **2016**, *57*, 4046.
[32] S.-J. Ji, Z.-Q. Jiang, J. Lu, T.-P. Loh, *Synlett* **2004**, *5*, 831.
[33] G. Shanthi, P. T. Perumal, *Tetrahedron Lett.* **2007**, *48*, 6785.
[34] J. Azuajea, C. R. Tubíoc, L. Escalantea, M. Gómezc, F. Guitiánc, A. Coelhoa, O. Caamaño, A. Gilc, E. Soteloa, *Appl. Catal. A Gen.* **2017**, *530*, 203.
[35] M. A. Bodaghifard, A. Mobinikhaledi, S. Asadbegi, *Appl. Organometal. Chem.* **2016**, *31*, 3577.
[36] (a) N. Azizi, A. Mobinikhaledi, A. Khajeh Amiri, H. Ghafuri, *Res. Chem. Intermed.* **2012**, *38*, 2271. (b) H. Niaz, H. Kashtoh, J. A. J. Khan, A. Khan, A.-T. Wahab, M. T. Alam, K. M. Khan, S. Perveen, M. I. Choudhary, *Eur. J. Med. Chem.* **2015**, *95*, 199.
[37] S. Ko, M. N. V. Sastry, C. Lin, C.-F. Yao, *Tetrahedron Lett.* **2006**, *46*, 5771.
[38] A. Kuraitheerthakumaran, S. Pazhamalai, M. Gopalakrishnan, *Chin. Chem. Lett.* **2011**, *22*, 1199.

[39] M. Maheswara, V. Siddaiah, Y. K. Rao, Y. M. Tzeng, C. Sridhar, *J Mol. Catal.* **2006**, *260*, 179.
[40] S. Ko, C. F. Yao, *Tetrahedron* **2006**, *62*, 7293.
[41] M. Inouye, T. Mio, K. Sumino, *Eur. J. Clin. Pharmacol.* **2000**, *56*, 35.
[42] J. Briede, D. Daija, M. Stivrina, G. Duburs, *Cell Biochem. Funct.* **1999**, *17*, 89.
[43] (a) M. F. Gordeev, D. V. Patel, E. M. Gordon, *J. Org. Chem.* **1996**, *61*, 924. (b) R. Boer, V. Gekeler, *Drugs Future* **1995**, *20*, 499. (c) S. Bahekar, D. Shinde, *Acta Pharm. (Zagreb). A* **2002**, *52*, 281.
[44] (a) F. Bossert, H. Mayer, E. Wehinger, *Angew. Chem. Int. Ed. Engl.* **1981**, *20*, 762. (b) P. K. Gilpin, L. A. Pachla, *Anal. Chem.* **1999**, *71*, 217. (c) S. Cosconati, L. Marinelli, A. Lavecchia, E. Novellino, *J Med. Chem.* **2007**, *50*, 1504.
[45] O. Prakash, K. Hussai, R. Kumar, D. Wadhwa, C. Sharma, K. R. Aneja, *Org. Med. Chem. Lett.* **2011**, *1*, 5.
[46] R. Guillen Sans, M. Guzman Chozas, *Pharmazie* **1988**, *43*, 827.
[47] T. J. El-Emary, E. A. Bakhite, *Pharmazie* **1999**, *54*, 106.
[48] A. Gangjee, H. D. Jain, J. Phan, X. Lin, X. Song, J. J. McGuire, R. L. Kisliuk, *J Med. Chem.* **2006**, *49*, 1055.
[49] M. Gholami Dehbalaei, N. Foroughifar, H. Pasdar, A. Khajeh-Amiri, *New J. Chem.* **2018**, *42*, 327.
[50] L. Kürti, B. Czakó, *Strategic Applications of Named Reactions in Organic Synthesis*, Elsevier Academic, Amsterdam **2005**, p. 286, 628.
[51] J. Giri, S. G. Thakurta, J. Bellare, A. K. Nigam, D. Bahadur, *J. Magn. Magn. Mater.* **2005**, *293*, 62.
[52] K. Azizi, M. Karimi, H. R. Shaterian, A. Heydari, *RSC Adv.* **2014**, *4*, 42220.
[53] K. Naka, A. Narita, H. Tanaka, Y. Chujo, M. Morita, T. Inubushi, I. Nishimura, J. Hiruta, H. Shibayama, M. Koga, S. Ishibashi, J. Seki, S. Kizaka-Kondoh, M. Hiraoka, *Polym. Adv. Technol.* **2008**, *19*, 1421.
[54] K. Can, M. Ozmen, M. Ersoz, *Colloids Surf. B* **2009**, *71*, 154.
[55] B. Luo, X. J. Song, F. Zhang, A. Xia, W. L. Yang, J. H. Hu, C. C. Wang, *Langmuir* **2010**, *26*, 1674.
[56] T. Zeng, L. Yang, R. Hudson, G. Song, A.-R. Moores, C.-J. Li, *Org. Lett.* **2011**, *13*, 442.

SUPPORTING INFORMATION

Additional supporting information may be found online in the Supporting Information section at the end of the article.

How to cite this article: Gholami Dehbalaei M, Foroughifar N, Khajeh-Amiri A, Pasdar H. *N*-propylbenzoguanamine sulfonic acid-functionalized magnetic nanoparticles: A novel and magnetically retrievable catalyst for the synthesis of 1,4-dihydropyridine derivatives. *J Chin Chem Soc*. 2018; 1–14. https://doi.org/10.1002/jccs.201800120